

CALL FOR PAPERS | *Small Vessels-Big Problems: Novel Insights into Microvascular Mechanisms of Diseases*

Blood capillary rarefaction and lymphatic capillary neoangiogenesis are key contributors to renal allograft fibrosis in an ACE inhibition rat model

 Péter Hamar¹ and Dontscho Kerjaschki²

¹Institute of Pathophysiology, Semmelweis University, Budapest, Hungary; and ²Institute of Pathology, University of Vienna, AKH, Vienna, Austria

Submitted 26 April 2016; accepted in final form 29 July 2016

Hamar P, Kerjaschki D. Blood capillary rarefaction and lymphatic capillary neoangiogenesis are key contributors to renal allograft fibrosis in an ACE inhibition rat model. *Am J Physiol Heart Circ Physiol* 311: H981–H990, 2016. First published August 5, 2016; doi:10.1152/ajpheart.00320.2016.—Chronic allograft fibrosis is the major cause of graft loss in kidney transplantation. Progression can only be reduced by inhibition of the renin-angiotensin system (RAS). We tested the hypothesis that the protection provided by angiotensin-converting enzyme (ACE) inhibition also decreases capillary rarefaction, lymphangiogenesis, and podocyte injury in allograft fibrosis. Fisher kidneys were transplanted into bilaterally nephrectomized Lewis rats treated with enalapril (60 mg/kg per day) (ACE inhibitor, ACEi) or vehicle. Proteinuria, blood urea nitrogen, and plasma creatinine were regularly assessed, and grafts were harvested for morphological and immunohistological analysis at various times up to 32 wk. In the vehicle group, many new lymphatic capillaries and severe and diffuse mononuclear infiltration of allografts were observed already 1 wk after transplantation. Lymphangiogenesis increased until *week 4*, by which time inflammatory infiltration became focal. Lymphatic capillaries were often located at sites of inflammation. Progressive interstitial fibrosis, glomerulosclerosis, capillary rarefaction, and proteinuria appeared later, at *weeks 4–12*. The number of lymphatic capillary cross sections strongly correlated with the interstitial fibrosis score. Podoplanin immunostaining, a marker of healthy podocytes, disappeared from inflamed or sclerotic glomerular areas. ACEi protected from lymphangiogenesis and associated inflammation, preserved glomerular podoplanin protein expression, and reduced glomerulosclerosis, proteinuria, tubulointerstitial fibrosis, and blood capillary rarefaction at 32 wk. In conclusion, ACEi considerably decreased and/or delayed both glomerulosclerosis and tubulointerstitial injury. Prevention of glomerular podoplanin loss and proteinuria could be attributed to the known intraglomerular pressure-lowering effects of ACEi. Reduction of lymphangiogenesis could contribute to amelioration of tubulointerstitial fibrosis and inflammatory infiltration after ACEi.

lymphangiogenesis; capillary rarefaction; chronic allograft fibrosis; glomerular podoplanin; angiotensin-converting enzyme inhibition

NEW & NOTEWORTHY

Beneficial effects of angiotensin-converting enzyme (ACE) inhibition in renal allograft fibrosis included preservation of podocyte podoplanin, reduction of proteinuria, and inhibition

Address for reprint requests and other correspondence: P. Hamar, Semmelweis University, Nagyvarad ter 4, Budapest, Hungary (e-mail: hamar.peter@med.semmelweis-univ.hu).

of tubulointerstitial fibrosis, lymphangiogenesis, and capillary rarefaction in rats. Reduction of lymphangiogenesis could contribute to amelioration of tubulointerstitial fibrosis and inflammatory infiltration after ACE inhibition.

ALLOGRAFT FIBROSIS IS A LEADING cause of posttransplant graft failure with still largely undiscovered pathomechanisms. Capillary rarefaction (8, 12) has been described in renal fibrosis previously (26). We hypothesized that rarefaction of blood capillaries is accompanied by simultaneous proliferation of lymphatic vessels. Capillary cross sections have been assessed previously with antibodies not differentiating between lymphatic endothelial cells (LECs) or blood capillary endothelial cells (BECs).

The Fischer-to-Lewis (F344-to-LEW) rat kidney allograft is the most frequently used animal model of chronic allograft fibrosis. The two inbred strains differ only in one myosin heavy chain (MHC) I antigen, and a number of non-MHC antigens. If ischemia is short (<25 min) during transplantation, an initial acute rejection episode resolves spontaneously without any immunosuppression but induces a chronic allograft fibrosis. Pathological proteinuria begins around 12 wk after grafting, eventually leading to allograft fibrosis (14, 29).

Our previous study has shown that, during the initial rejection episode, radioactively labeled recipient lymphocytes infiltrate the graft temporarily and leave the graft shortly after infiltration. Labeled lymphocytes were found in the tubulointerstitium, suggesting that lymphocyte migration out of the graft could take place through lymphatic vessels (14). The role of lymphatic capillaries in the organization of inflammatory infiltration (6, 21) and fibrosis (10) has been suggested before. In this model, we did not observe signs of alloimmune-mediated injury with electron microscopy 32, 40, and 52 wk after transplantation, suggesting that the alloimmune process may cease during the late phase of chronic allograft fibrosis (32). The predominance of alloantigen-independent processes in the late phase of allograft fibrosis is also supported by retransplantation experiments (32). Following cessation or reduction of alloimmune processes, an alloantigen-independent mechanism may be primarily responsible for the self-perpetuation and progression of allograft fibrosis (15, 17).

Involvement of the renin-angiotensin system (RAS) is well documented in renal fibrosis, and RAS inhibition is the only approved treatment to slow progression of renal fibrosis (9, 16, 27, 35). RAS inhibition may act by reducing glomerular capillary pressure increase caused by hyperfiltration of remnant

Table 1. *Body weight (g)*

Week	0	1	4	8	16	24	32
Healthy	207 ± 13	279 ± 27	318 ± 18	358 ± 39	407 ± 48	507 ± 68	546 ± 72
16 wk	183 ± 45	264 ± 15	303 ± 35	330 ± 71	350 ± 82		
TX _{ACEi}	206 ± 22	295 ± 21	309 ± 27	348 ± 22	401 ± 32	435 ± 32*	465 ± 31*
TX _{NoTh}	210 ± 27	290 ± 24	304 ± 25	336 ± 22	334 ± 28*	346 ± 26†	350 ± 57†

Values are means ± SD. In the 16-week experiment, only animals that survived ≤16 wk are included. **P* < 0.05, †*P* < 0.001 vs. healthy (ANOVA). TX_{ACEi}, 32-wk-old allografts with angiotensin-converting enzyme inhibitor treatment. TX_{NoTh}, 32-wk-old allografts with no treatment.

nephrons (5), and RAS inhibition may reduce extracellular matrix accumulation by decreasing matrix production and stimulating matrix degradation (7, 17, 36).

In the present study, we evaluated tubulointerstitial fibrosis, inflammation, and glomerulosclerosis up to 32 wk after Fisher-to-Lewis allograft transplantation. The focus of the study was to follow lymphatic neoangiogenesis and blood capillary rarefaction, and the morphological changes were correlated with changes in blood urea concentration and urinary protein excretion. To reveal the role of RAS in the above changes, one group of rats was treated with enalapril.

MATERIALS AND METHODS

Experimental animals. Naive male inbred Lewis (LEW, RT¹) and Fisher (F-344, RT^{1v1}) rats (2) at 8 wk of age were used throughout the experiment. All animals were obtained from Charles River Germany, through Akrom Kft (Budapest, Hungary). The rats were housed under standard conditions and received rat chow and water ad libitum. All experimental procedures were in accordance with the *Guide for the Care and Use of Laboratory Animals* published by the US National Institutes of Health (NIH publication No. 85-23, revised 1996), and the experimental protocol was reviewed and approved by the Institutional Ethical Committee for Animal Care and Use of Semmelweis University (approval number: XIV-I-001/2012-4/2012).

Renal transplantation, follow-up of graft function, and end points. Fisher rats served as donors and Lewis rats as recipients. Transplantation was performed as previously described (32). Briefly, the animals were anesthetized with pentobarbital sodium (Nembutal, 50 mg/kg, ip) and atropine sulfate (0.05 mg/kg) (18, 37). The left donor kidney was perfused with 4°C cold ringer lactate, removed, and positioned orthotopically into the recipient, whose renal vessels had been isolated and clamped with the left native kidney removed. End-to-end anastomosis of renal artery, vein, and ureter was performed using 10-0 prolene sutures. Total graft ischemia was set to 25 min. No immunosuppression was applied. Aseptic conditions were maintained throughout all surgical procedures. Postoperative care included morphine hydrochloride (2.5 mg/kg body wt, sc after the operation) analgesia, and, to prevent infectious complications during the perioperative phase, rats received 20 mg/kg per day Cephtriaxone (Rocephine) sc. (Roche Hungary, Budaörs, Hungary) during the first 10 postoperative days, at which time the right native kidney was removed.

Animals were placed in metabolic cages (Techniplast, Buguggiate, Italy) for 24 h every 4 wk for the estimation of proteinuria. Body

weight was measured, and blood was taken from the tail vein by the end of the urine collection period to measure blood urea nitrogen (BUN) and plasma creatinine. Serum and urine samples were stored at -80°C for later measurements. Urinary total protein concentrations were determined by the biuret method (Bio-Rad Laboratories, Munich, Germany). Absorbance was determined at 595 nm with a Philips PU8700 spectrophotometer. BUN and creatinine concentrations were determined photometrically with a Reflotron IV automat (Boehringer, Mannheim, Germany).

Experiments were terminated at different time points up to 32 wk. Under isoflurane narcosis (30, 42), rats were exsanguinated from the abdominal aorta, and kidney grafts were removed, cut, and fixed in 4% buffered formalin and embedded in paraffin (FFPE). All histopathological procedures were performed on paraffin-embedded sections.

Experimental design. Fischer-to-Lewis (F344-to-LEW) rat kidney allografts were investigated in two experimental settings. Nontransplanted naive Lewis rats at 8 wk of age were included as controls (*n* = 4).

In the first series, grafts were investigated 32 wk after engraftment to study capillary rarefaction and lymphangiogenesis with BEC- and LEC-specific antibodies (JG12 aminopeptidase and LF3 podoplanin, respectively). Transplanted animals received either usual drinking water (no therapy group, TX_{NoTh}; *n* = 4) or an angiotensin-converting enzyme (ACE) inhibitor (ACEi) enalapril (Merck Sharp and Dohme, Whitehouse Station, NJ) (60 mg/l ACEi group, TX_{ACEi}; *n* = 4) throughout the study period.

In the second series, untreated allografts were harvested 1, 2, 4, or 16 wk after engraftment (*n* = 4/time) to investigate the time course and progression of allograft fibrosis, the podoplanin expression in glomeruli, the lymphangiogenesis, and lymphocytic infiltration.

Histology. For histology, FFPE kidney sections were stained with hematoxylin/eosin (HE), periodic acid-Schiff (PAS), or acid fuchsin orange-G (SFOG) to quantify fibrosis as protein deposits (1). We quantified the extent of glomerular sclerosis (GSI), interstitial fibrosis (IF), tubular atrophy (TA), and tubulointerstitial inflammation (TII) according to the BANFF scoring system (33, 34). Glomerulosclerosis was defined as an increase in glomerular mesangial matrix, focal adhesions to the Bowman's capsule, or collapse of the glomerular capillaries (12). Slides were scored in a blinded fashion, semiquantitatively from 0 to 4 [0: no histopathologic change; 1: mild, <25%; 2: moderate, 25–50%; 3: severe, >50%; 4: very severe change, >75% of the analyzed structures (glomeruli, tubules, interstitial fields) show pathologic changes (GSI, IF, TA, TII)] (35). Additionally, the percentage of normal glomeruli is given. A minimum of 50 glomeruli or

Table 2. *Proteinuria (mg/24 h)*

Week	4	8	12	16	20	24	28	32
Healthy	27 ± 15	28 ± 11	33 ± 8	40 ± 10	45 ± 13	30 ± 8	43 ± 11	40 ± 9
16 wk	37 ± 13	20 ± 3	59 ± 13*	86 ± 15†				
TX _{ACEi}	16 ± 3	31 ± 10	34 ± 14	49 ± 9	43 ± 9	54 ± 12*	78 ± 19†	110 ± 12†
TX _{NoTh}	21 ± 6	47 ± 6	62 ± 15*	114 ± 16†	177 ± 24†	170 ± 28†	257 ± 35†	246 ± 43†

Values are means ± SD. In the 16-week experiment, only animals that survived ≤16 wk are included. **P* < 0.05, †*P* < 0.001 vs. healthy (ANOVA).

Table 3. BUN retention (mg/dl)

Exp. Group	1	4	8	16	20	24	28	32
Healthy	13 ± 5	20 ± 6	22 ± 8	19 ± 11	24 ± 6	17 ± 3	21 ± 9	20 ± 7
1 wk	20 ± 5							
16 wk	17 ± 2	30 ± 6	29 ± 7	38 ± 13*				
T _X ACEi	15 ± 3	21 ± 2	32 ± 7	28 ± 4	25 ± 6	41 ± 9†	38 ± 14*	53 ± 22†
T _X NoTh	22 ± 4	18 ± 2	33 ± 9	61 ± 12†	102 ± 7†	88 ± 16†	134 ± 9†	152 ± 9†

Values are means ± SD. **P* < 0.01, †*P* < 0.001 vs. healthy (ANOVA). BUN, blood urea nitrogen.

20 fields of view (fv) per kidney was evaluated at ×400 magnification.

Antibodies and immunohistochemistry reagents. Monoclonal antibodies against macrophages (ED-1) were purchased from Serotec Camon Labor-Service (Wiesbaden, Germany). Lymphocytes were detected with CD45R (B cells) and CD43 (T cells). Endothelial cells were labeled with LF3 podoplanin found on LECs and podocytes or JG12, an aminopeptidase, found on vascular (blood) endothelial cells (25). Color reactions were performed with commercial kits for 3-amino-9-ethylcarbasol (brick red) (ID Laboratories, London, Ontario, Canada), diaminobenzidine (brown) (Perbio 9b; Pierce, Rockford, IL), vector-blue (blue) (Vector Laboratories, Burlingame, CA), and vector-red (red) (Vector Laboratories).

Immunohistology. Immunohistochemistry was performed on FFPE slides. Following deparaffination, antigens were retrieved in an autoclave (20 min, 1.2 Bar, citrate buffer). The avidin-biotin method was used. Signals were retrieved with streptavidin and horseradish or alkaline phosphatase methods. Samples were counterstained with Giemsa. Lymphatic cross sections or cells staining positive were counted and expressed as lymphatic capillaries or cells per fv. At least 20 fv sections per specimen were counted at ×400 magnification.

Statistics. Results are presented as means ± SD. The normality of data was checked by Shapiro-Wilk *W*-test, and homogeneity of variances was checked by Bartlett's test. Continuous variables were compared using one-way ANOVA, followed by Dunnett's multiple-comparison post hoc test vs. healthy rats. Discrete variables were compared by Kruskal-Wallis test followed by Dunn's multiple-comparison test vs. healthy rats. Urinary protein excretion and BUN were tested using two-way ANOVA for repeated measures with Tukey's and Sidak's multiple-comparison tests. Data at 32 wk in the T_XACEi and T_XNoTh groups were compared using Student's unpaired *t*-test or Mann-Whitney *U*-test. Linear correlation was assessed by Pearson product-moment correlation coefficient. The null hypothesis was rejected if the *P* value reached statistical significance (*P* < 0.05).

RESULTS

Functional studies. Body weight increased during the observation period. Weight gain was slower in the T_XNoTh group vs. the T_XACEi group from week 16 (Table 1).

In all recipients, proteinuria progressed over time (Table 2). Pathological proteinuria started to develop at week 12 in untreated animals. Proteinuria initiated later and progressed slower in the T_XACEi group.

Table 4. Plasma creatinine retention (μmol/l)

Exp. Group	1	4	8	16	20	24	28	32
Healthy	<44	<44	<44	<44	<44	<44	<44	<44
16 wk	<44	<44	<44	49 ± 4				
T _X ACEi	<44	<44	<44	<44	<44	<44	<44	60 ± 13
T _X NoTh	<44	<44	<44	56 ± 6	62 ± 10	86 ± 27*	91 ± 42*	141 ± 44*

Applicable values are means ± SD. **P* < 0.001 vs. healthy (ANOVA).

The deterioration of renal function further manifested in elevated BUN. BUN retention reached pathological range only 16–20 wk after transplantation, and the most severe retention was in the T_XNoTh group (Table 3).

Plasma creatinine was below the detection limit of the Reflotron method (<44 μmol/l) during the first 16 wk of the study. Plasma creatinine started to rise at week 16 in the T_XNoTh group but reached detectable levels in the T_XACEi group only on week 32 (Table 4).

Light microscopy and immunohistology: Inflammation and fibrosis of the allografts. In the time-course experiment on SFOG- and PAS-stained slides (Table 5, Fig. 1) at week 1, severe, diffuse mononuclear infiltration was the predominant finding. Mononuclear infiltration was occasionally accompanied by interstitial edema. Interstitial edema was detected as unstained, clear areas between tubuli with filamentous structures in inflamed areas. Signs of fibrosis were absent at week 1. At week 2, infiltration was still diffuse in some grafts but became focal in others. Tubuli themselves, however, were not visibly damaged. Sclerosis of glomeruli (FSGS) was focal if present. FSGS and TA progressed by week 4. Fibrotic matrix appeared (IF) in the interstitium; however, inflammatory infiltration did not change significantly. At week 8, IF, TA, and FSGS became severe and progressed further by week 16, whereas inflammatory infiltration remained focal.

PAS and SFOG staining of 32-wk-old grafts (Table 5, Fig. 1) revealed focal sclerosis (grade I–II) of glomeruli in the T_XACEi group compared with a more global (grade III–IV) sclerosis in the T_XNoTh group. Most glomeruli showed some sclerosis in the T_XNoTh group, whereas many glomeruli were still normal appearing in T_XACEi grafts. IF was mild or absent in T_XACEi grafts in contrast to significant IF in T_XNoTh. Many tubuli were severely atrophic with flat epithelial cells, and hyaline-filled tubular cross sections were common in the T_XNoTh but not in the T_XACEi group. Inflammatory foci were seldom in the T_XACEi group, but mononuclear infiltration was common and diffuse in T_XNoTh rats.

Type of interstitial capillaries. Double immunostaining of 32-wk-old allografts for podoplanin (LF3) on LECs and podocytes and aminopeptidase (JG12) on BECs (Table 6, Fig. 2)

Table 5. *Allograft fibrosis and inflammation*

Group	Time	Normal Glomeruli, %	GSI Score	IF Score	TA Score	TII Score
Healthy		98.0 ± 1.0	0.1 ± 0.1	0.0 ± 0.1	0.1 ± 0.1	0.2 ± 0.1
16 wk	1 wk	82.0 ± 17.0	0.4 ± 0.1	0.1 ± 0.1	0.2 ± 0.1	3.4 ± 0.4
	2 wk	47.0 ± 11.0	1.4 ± 0.2	0.3 ± 0.2	0.8 ± 0.4	2.2 ± 0.6
	4 wk	12.0 ± 2.0	2.1 ± 0.4	1.8 ± 0.3	1.3 ± 0.5	1.6 ± 0.6
	8 wk	4.0 ± 4.0	3.4 ± 0.3	2.0 ± 0.8*	2.2 ± 0.6*	1.3 ± 0.7*
	16 wk	6.0 ± 3.0	3.1 ± 0.5	2.4 ± 0.8†	2.5 ± 0.5†	1.1 ± 0.3†
Tx _{ACEi}	32 wk	18.0 ± 3.0	1.8 ± 0.2	1.0 ± 0.1	0.9 ± 0.1	0.8 ± 0.1
Tx _{NoTh}		0.0	3.6 ± 0.4	2.5 ± 0.4*‡	2.7 ± 0.2*‡	1.9 ± 0.3‡

Values are means ± SD. Scores are based on 50 glomeruli or 20 fields of view at ×400. **P* < 0.05, †*P* < 0.01 vs. healthy, ‡*P* < 0.05 vs. Tx_{ACEi}. GSI, glomerular sclerosis; IF, interstitial fibrosis; TA, tubular atrophy; TII, tubulointerstitial inflammation.

demonstrated a significantly higher number of lymphatic and lower number of blood capillary cross sections in the Tx_{NoTh} group compared with healthy native kidneys or Tx_{ACEi} grafts. Blood capillaries were reduced in number,

and the regular appearance of peritubular capillaries was lost as diameter inhomogeneity and tortuosity of JG12-positive capillaries were observed in fibrotic areas of allografts in the Tx_{NoTh} group.

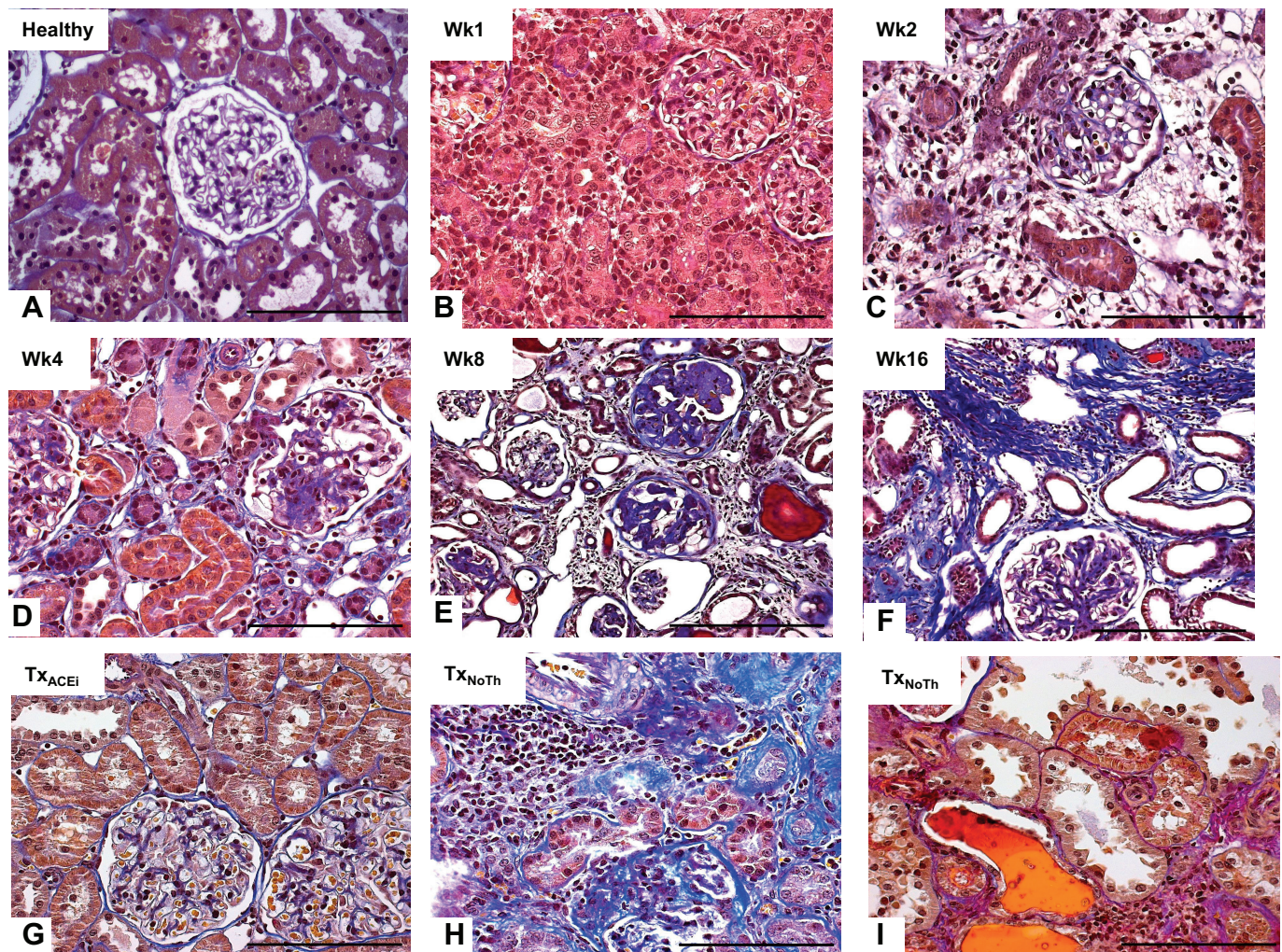


Fig. 1. Evolution of tubulointerstitial fibrosis and inflammation up to 32 wk after transplantation. Fischer-to-Lewis (F344-to-Lew) allografts 1, 2, 4, 8, 16, and 32 wk after engraftment are shown with acid fuchsin orange-G staining; magnification ×400, scale bar = 100 μm. *A*: healthy rat kidney. *B*: week 1. Severe interstitial inflammatory infiltration is seen, with no signs of fibrosis. *C*: week 2. Varying severity or focal interstitial infiltration and interstitial edema (pale areas between tubular cross sections) are seen. Extracellular matrix deposition is in parts of glomeruli. *D*: week 4. Focal interstitial inflammation and matrix deposition (interstitial fibrosis, IF) are shown with low-grade (grade I–II) sclerosis of glomeruli (FSGS) in some glomeruli. *E*: week 8. Severe IF and tubular atrophy (TA) with extensive cast formation are seen, with sclerotic or collapsed glomeruli (grade III–IV). *F*: week 16. Extensive IF and TA are seen. Casts are in tubuli. *G*: week 32 (transplanted animal group with angiotensin-converting enzyme inhibitor, Tx_{ACEi}); FSGS grade: I, mild tubulointerstitial fibrosis. *H* and *I*: week 32, transplanted animal group with no therapy (Tx_{NoTh}). These groups had almost completely obliterated glomeruli (FSGS grade IV), severe IF, and severe tubulointerstitial inflammatory infiltration (TII). *I*: TA and hyaline-filled tubular cross sections are seen.

Table 6. Immunostaining: Lymphatic and blood capillary cross sections and podoplanin-negative glomeruli

Group	Time	Lymphatic Cross Sections/fv	Blood Capillary Cross Sections/fv	LF3-Negative Glomeruli, %
Healthy		1.2 ± 0.3	25.0 ± 3.0	3.0 ± 2.0
16 wk	1 wk	7.0 ± 3.0	21.0 ± 5.0	2.0 ± 1.0
	2 wk	10.0 ± 6.0*	18.0 ± 4.0	11.0 ± 4.0
	4 wk	8.0 ± 6.0	6.0 ± 5.0	25.0 ± 8.0
	8 wk	11.0 ± 5.0*	7.0 ± 6.0	29.0 ± 9.0
	16 wk	13.0 ± 7.0†	5.0 ± 4.0	44.0 ± 6.0†
TX _{ACEi}	32 wk	5.0 ± 3.0	11.0 ± 9.0	57.0 ± 9.0†
TX _{NoTh}		11.0 ± 4.0*‡	4.0 ± 4.0	83.0 ± 5.0*‡‡

Values are means ± SD. Lymphatic endothelial cell (LF3 podoplanin) and blood capillary endothelial cell (JG12 aminopeptidase) staining was conducted. * $P < 0.05$, † $P < 0.01$ vs. healthy kidneys. ‡ $P < 0.05$ vs. TX_{ACEi}. fv: field of view at ×400.

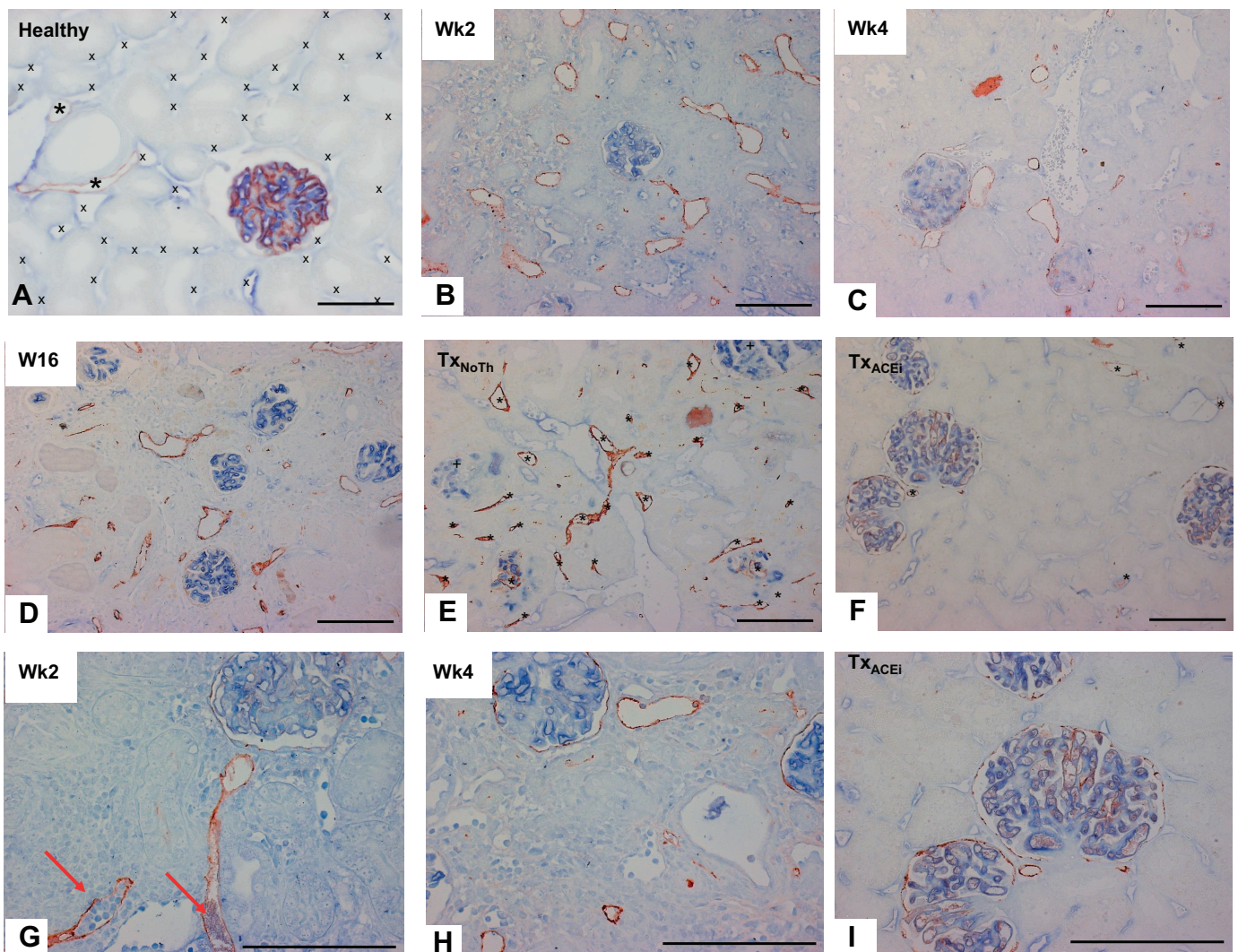


Fig. 2. Changes in the density of peritubular and lymphatic capillaries up to 32 wk after transplantation. F344-to-Lew allografts 2, 4, 16, and 32 wk after engraftment are shown with double immunostaining. An overview of interstitial capillary types (A–F, magnification ×200) is provided. Glomeruli and a lymphatic capillary with inflammatory cells (G–I, magnification ×400, scale bar = 100 μm) are seen. LF3:podoplanin (1:1,000) on podocytes and lymphatic capillaries (3-amino-9-ethylcarbasol, AEC; brick red) + JG12:aminopeptidase (vector blue) are shown. A: healthy rat kidney. Two lymphatic (*) and 41 blood (x) peritubular capillary cross sections are shown. B–D: weeks 2, 4, and 16. In several lymphatic capillary cross sections and peritubular capillary rarefaction, peritubular capillaries become irregular in shape and distribution and less in number. E: week 32, TX_{NoTh}. Many (25) lymphatic (*) capillaries, severely dilated peritubular capillaries, and peritubular capillaries are irregular in size and distribution. Almost completely obliterated glomeruli (+, FSGS grade IV) with missing podoplanin staining are shown. F: week 32, TX_{ACEi}. Lymphatic capillaries are rare (5), and peritubular capillaries appear in regular fashion like in a healthy kidney. Glomerular podoplanin staining is present. G–I: glomeruli became podoplanin negative already at weeks 2 (G) and 4 (H), but glomerular podoplanin was preserved to some extent in TX_{ACEi} (I). G: mononuclear infiltration and 2 lymphatic capillary cross sections in the interstitium. Lymphatic capillaries are shown with mononuclear cells (arrow).

Investigating the grafts at earlier times with (LF3) immunostaining (Table 6, Fig. 3) or double staining (Fig. 2) demonstrated that already 1 wk after transplantation numerous LF3+ lymphatic capillaries appeared in the tubulointerstitium. Lymphatic capillaries were often associated with mononuclear infiltration (lymphangiogenesis with nodular infiltrates) (Fig. 4). Thereafter, lymphatic cross sections with nodular infiltrates were present throughout the 16-wk observation period. The number of lymphatic capillary cross sections correlated with the severity of tubulointerstitial fibrosis (IF score) (Fig. 6). Aminopeptidase (JG12)-positive blood capillaries were present in high numbers still 2 wk after transplantation but were significantly reduced and irregular thereafter (Fig. 2). On the other hand, ACE inhibition preserved the morphology and number of peritubular capillaries (Fig. 2H).

Type of inflammatory infiltration. Investigating the time course of triple immunostaining for T and B lymphocytes and podoplanin revealed that mononuclear infiltrating cells were mostly T (CD43+) and less B (CD45R+) lymphocytes and only a few macrophages (ED1+) (Fig. 5) in nonimmunosuppressed F344-to-LEW renal allografts.

Mononuclear infiltration was most severe and diffuse at *day 7*, at which time T cells were predominant. Infiltration became focal in most allografts at *day 14* when B cells also appeared in large numbers. One month after transplantation mononuclear infiltration became focal and contained numerous B cells besides T lymphocytes.

In 32-wk-old allografts, focal mononuclear infiltrations were accompanied by LF3+ lymphatic capillary cross sections (Fig. 6). Some lymphatic capillaries contained various numbers of

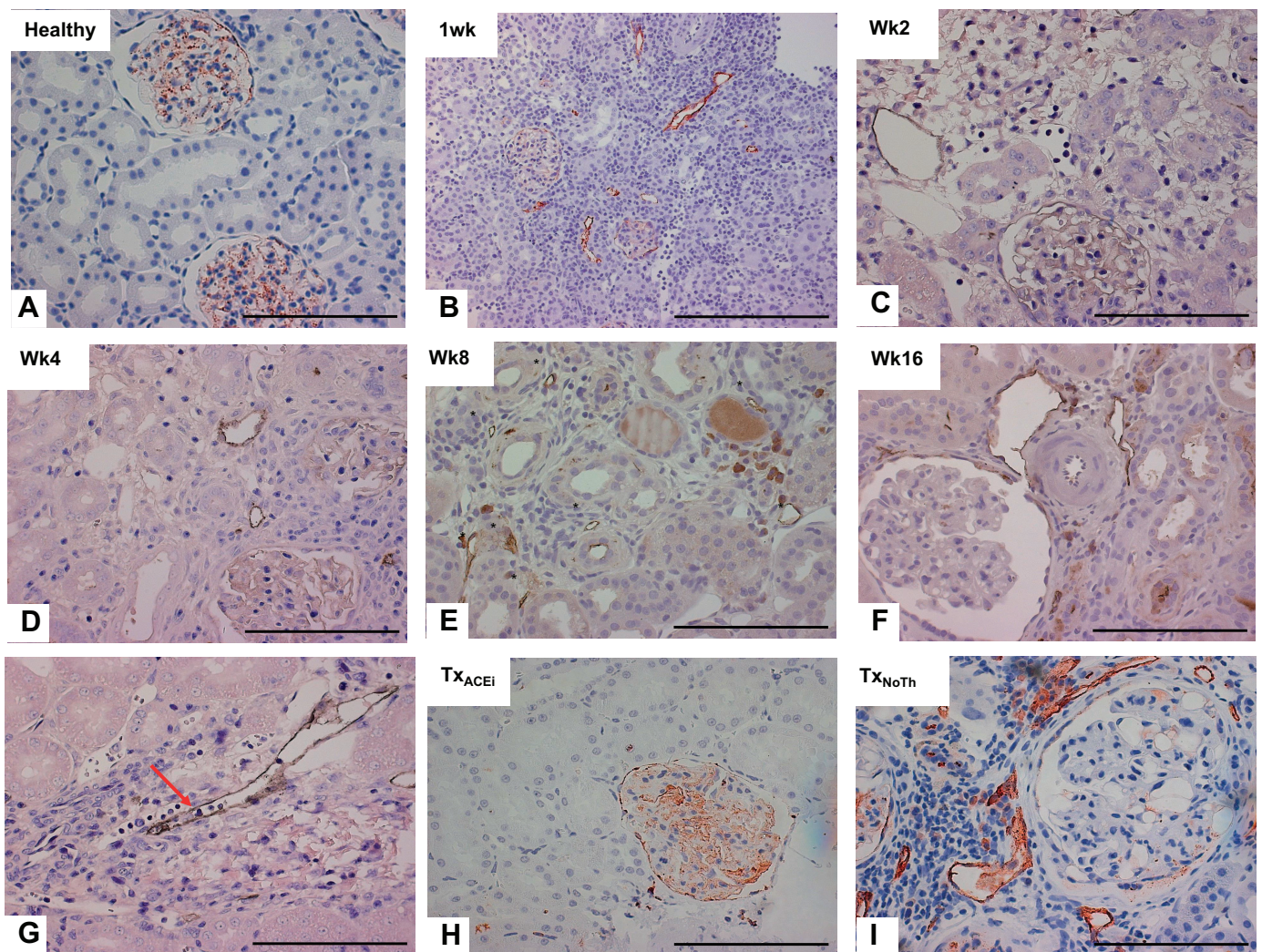


Fig. 3. Changes in the immunohistochemical staining of podoplanin in glomeruli and lymphatic capillaries up to 32 wk after transplantation. F344-to-Lew allografts 1, 2, 4, 8, 16, and 32 wk after engraftment are shown with magnification $\times 400$; scale bar = 100 μm . LF3 (podoplanin on podocytes and lymphatic capillaries is shown; diaminobenzidine, DAB, is brown). *A*: normal kidney. Podoplanin-positive glomeruli and no lymphatic capillaries are seen. *B*: *week 1*. Severe, diffuse inflammatory infiltration with lymphatic capillary cross sections in the interstitium is seen. *C*: *week 2*. Focal infiltration with edema and lymphatic capillaries is seen. Partially sclerotic glomerulus with podoplanin positivity is in the healthy part. *D*: *week 4*. Reduced glomerular podoplanin staining in 2 glomeruli and moderate interstitial inflammation with 3 lymphatic cross sections are seen. *E*: *week 8*. Eight lymphatic cross sections, interstitial inflammation, and tubular hyaline are shown. *F*: *week 16*. Podoplanin-negative glomerulus and lymphatic capillaries in the interstitium with mononuclear infiltration are shown. *G*: lymphatic capillary with infiltrating mononuclear cells (arrow) (2 wk after engraftment). *H*: *week 32*, TX_{ACEI}. Podoplanin-positive glomerulus and normal interstitium are shown. *I*: *week 32*, TX_{NoTh}. Podoplanin-negative glomerulus, focal inflammation, and several (14) lymphatic capillaries are shown.

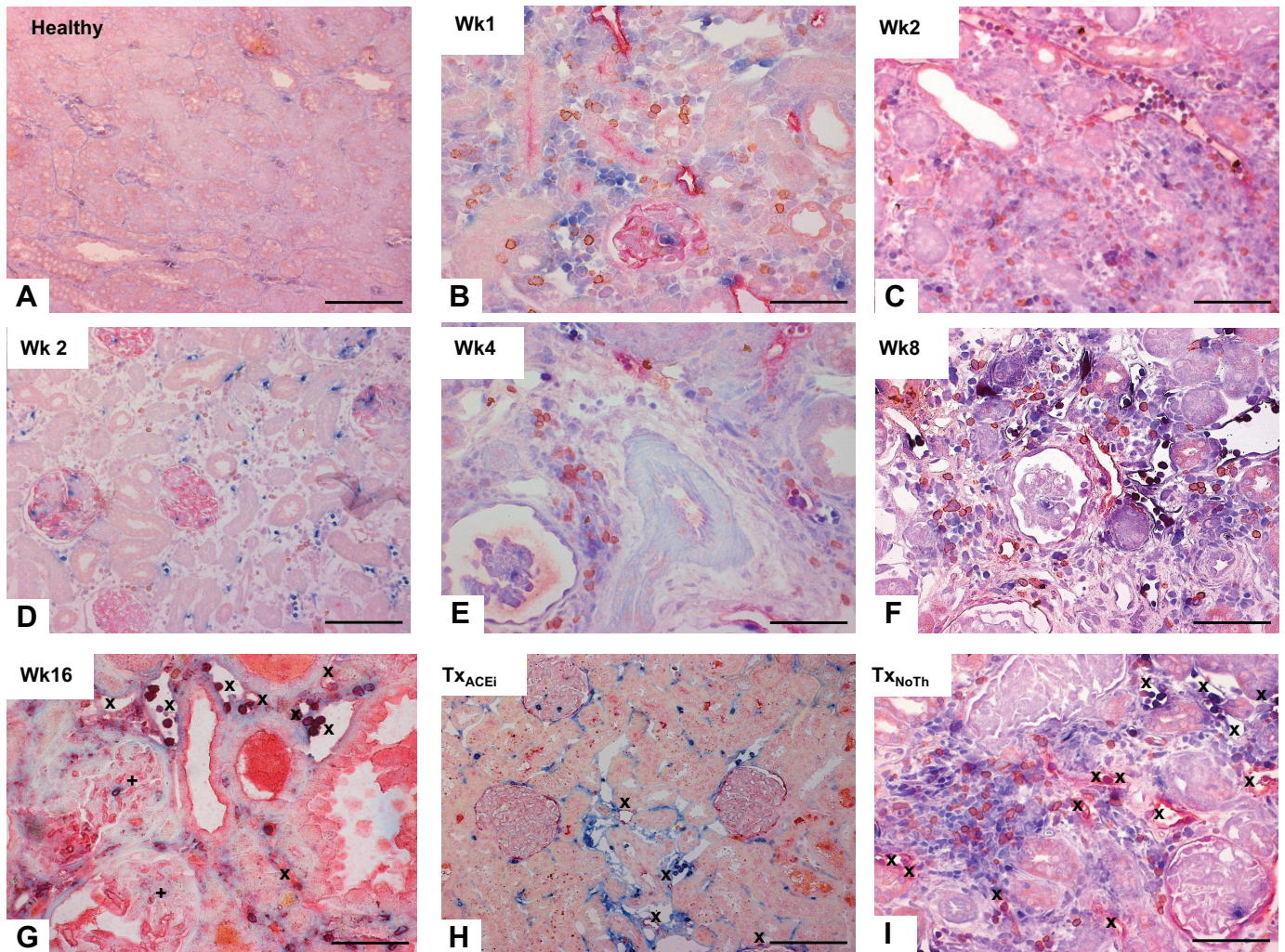


Fig. 4. Immunohistochemistry of mononuclear (CD43 and CD45R) infiltration up to 32 wk after transplantation. F344-to-Lew allografts 2, 4, and 8 wk after engraftment are shown. Triple immunostaining was performed, with magnification $\times 200$; scale bar = 100 μm . LF3 (podoplanin on podocytes and lymphatic capillaries, vector red), CD43 (T cells, vector blue), and CD45R (B cells, AEC, which is brick red) are shown. A: normal interstitium in a healthy rat. B: week 1. Severe, diffuse mononuclear infiltration with B (brick red) and T cells (blue) is shown. Cross sections of lymphatic capillaries (red) are shown. Glomeruli have podoplanin staining (red). C and D: week 2. Focal infiltration adjacent to lymphatic capillaries (B) is shown. Despite mild interstitial infiltration and edema, glomeruli are podoplanin (LF3) positive. E: week 4. Severe glomerular sclerosis (grade IV) and severe tubulointerstitial infiltration with T and B cells are shown. F: week 8. Focal inflammation with lymphatic cross sections is shown. Glomeruli are podoplanin (LF3) negative. G: week 16. Atrophic tubuli, hyaline cylinders and glomeruli are partially stained with LF3. Infiltrating cells are both T and B lymphocytes. Lymphatic capillaries (x) with T lymphocytes in lumen are shown. H: week 32, TX_{ACEi} . Glomeruli are podoplanin positive. Inflammatory cells are both T and B lymphocytes; 4 lymphatic capillary cross sections (x) are seen. I: week 32, TX_{NoTh} . Podoplanin-negative glomerulus is seen. Severely infiltrated area and 13 lymphatic capillary cross sections (x) are seen. Infiltrating cells are both B cells and T cells.

mononuclear cells in their lumen. The inflammatory infiltrates were still mostly CD43+ T lymphocytes both at 8 and 32 wk after engraftment, and most of the infiltrating cells were ED-1 negative both in the TX_{NoTh} and TX_{ACEi} groups.

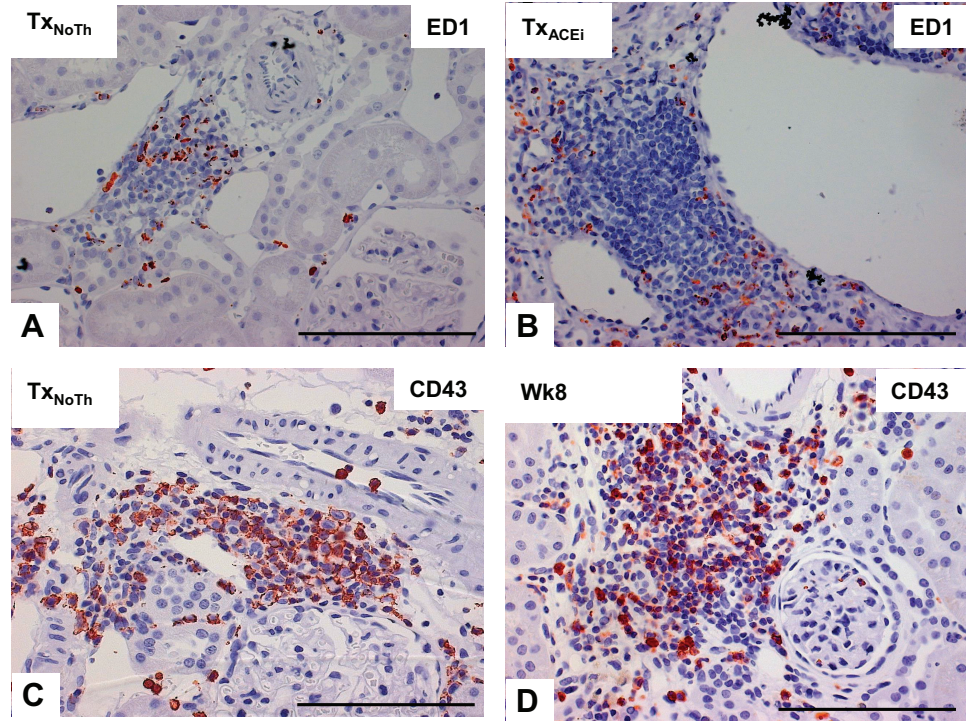
Glomerular podoplanin staining. In healthy rat kidneys (Fig. 2A), glomerular capillaries have a double-positive contour for both the blood (aminopeptidase JG12) and the lymphatic (podoplanin LF3) endothelial markers. At sites of inflammatory infiltration, glomeruli were LF3 (podoplanin) negative already 1 wk after transplantation (Figs. 2 and 3). Besides areas of interstitial infiltration, sclerotic areas of glomeruli were also podoplanin negative (Figs. 2 and 3). In 32-wk-old allografts, most of the glomeruli were podoplanin negative in the TX_{NoTh} group, whereas more glomeruli expressed some podoplanin in

the TX_{ACEi} group (Table 6). The ratio of unstained glomeruli correlated closely with proteinuria (Fig. 7).

DISCUSSION

The main finding of the study was that the F344-to-LEW chronic allograft fibrosis model can be characterized by lymphangiogenesis accompanied by nodular tubulointerstitial lymphocyte infiltration and fibrosis as well as a gradual loss of podoplanin from glomeruli. Besides areas of nodular interstitial inflammation, lymphatic capillaries were observed around sclerotic glomeruli; thus lymphatic capillaries may be involved in inflammatory and fibrotic processes. The observed rarefaction of peritubular capillaries may contribute to the progression

Fig. 5. Scarce macrophage but intense T-cell infiltration at 8 and 32 wk after transplantation. F344-to-Lew allografts 32 and 8 wk after engraftment are shown. Immunostaining, with magnification $\times 400$ was performed; scale bar = 100 μm . ED1 (macrophage marker, vector red), CD43 (T cells, DAB, brown) was used. *A* and *B*: week 32. Foci of mononuclear infiltration were mostly ED1 negative in both the No Therapy (*A*) and ACEi (*B*) groups. *C* and *D*: CD43 staining (DAB) of 32-wk-old (*C*) and 8-wk-old (*D*) allografts. Most infiltrating cells are CD43 positive T cells.



of fibrosis by inducing hypoxia, as reviewed recently (12). As angiotensin II induces vascular dysfunction (22), antifibrotic benefits of ACE inhibition may be attributed to prevention of blood capillary rarefaction (3).

Lymphangiogenesis as a contributor to renal fibrosis is well established (19). Similar lymphangiogenesis with nodular infiltrates has been described in kidney fibrosis also in the remnant kidney model (25) and in human kidney allografts (10). The novelty of our study is the demonstration of lymphangiogenesis with nodular infiltrates in the F344-to-LEW allograft model of chronic allograft fibrosis. Furthermore, the correlation of lymphatic neoangiogenesis with nodular infil-

trates and the severity of allograft fibrosis is described here for the first time. Similar progressive rarefaction of blood capillaries was associated with renal fibrosis, and the antifibrotic effects of angiotensin antagonism were attributed to preservation of renal blood capillaries recently (31). However, the importance of blood capillaries in allograft fibrosis has not been demonstrated before.

Proteinuria, BUN, and creatinine were similar to previously reported data in control animals (11, 27). Better-preserved renal function and less proteinuria manifested in better preserved body weight gain in ACEi-treated rats. Proteinuria has been suggested to induce tubulointerstitial lymphangiogenesis (40) before the onset of interstitial inflammation and fibrosis (39). Proteinuria-induced lymphangiogenesis could explain the observed increase in interstitial lymphatic neoangiogenesis in our proteinuric rats. Lymphatic capillaries were predominantly

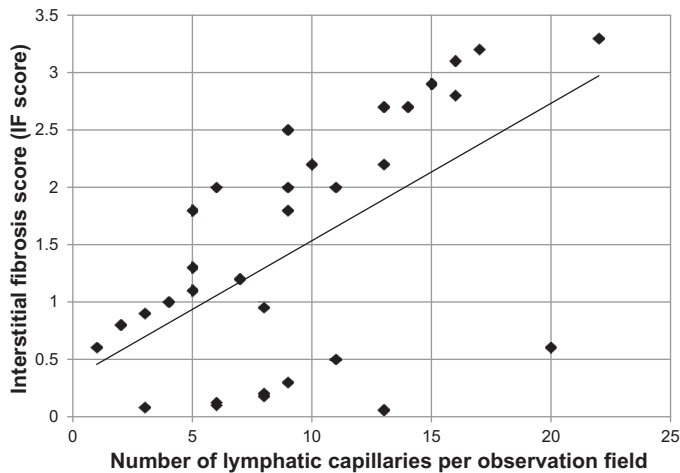


Fig. 6. Correlation between the number of lymphatic capillary cross sections (LF3) and IF score. LF3-positive lymphatic capillary cross sections were counted per field of view under $\times 400$ magnification and correlated with the semiquantitative IF score. Correlation statistics: $y = 0.1198x + 0.337$. $R^2 = 0.3475$.

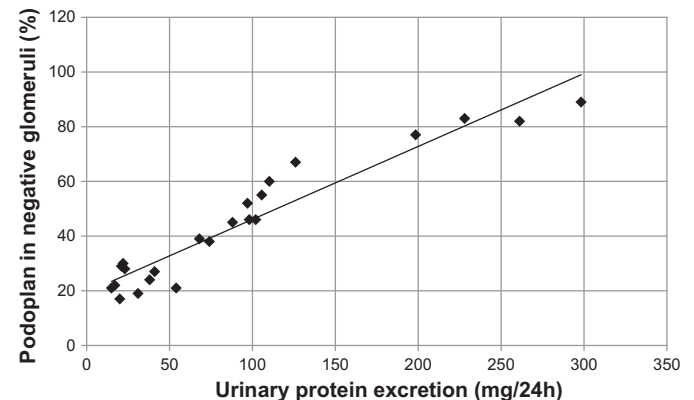


Fig. 7. Correlation between the percentage of podoplanin-negative glomeruli and daily urinary protein excretion. Correlation statistics: $y = 0.2668x + 19.43$. $R^2 = 0.9119$.

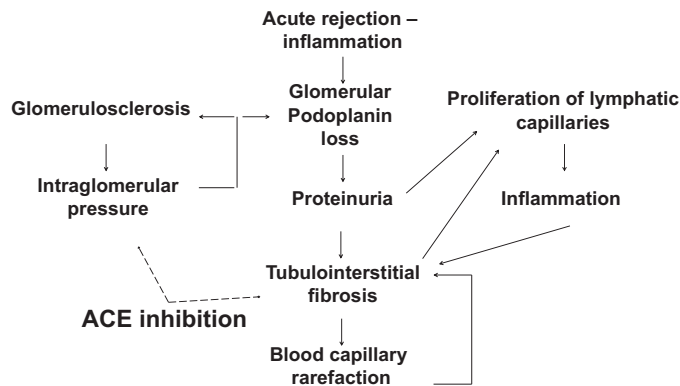


Fig. 8. Mechanisms of the acute rejection-induced allograft fibrosis. One week after transplantation, severe, diffuse tubulointerstitial inflammation was observed as a histological whole mark of acute rejection. Inflammation was associated with glomerular sclerosis, podoplanin loss, and proliferation of lymphatic capillaries. Glomerular podoplanin loss correlated with proteinuria, which has been suggested to induce proliferation of lymphatic capillaries and tubulointerstitial fibrosis. Tubulointerstitial fibrosis can cause blood capillary rarefaction, which in turn can worsen fibrosis attributable to tissue hypoxia. ACE inhibition has been described to reduce intraglomerular pressure and inhibit fibrosis.

observed in inflamed areas. Thus lymphatic neoangiogenesis may be triggered by proteinuria, but the strong association of lymphatic neoangiogenesis with inflammatory infiltration of the tubulointerstitium suggests a possible active role of lymphatic capillaries in inflammation. Indeed, lymphangiogenesis influences the progression of fibrosis by promoting inflammatory infiltration (13, 23). Also, lymphangiogenesis can develop as a consequence of fibrosis (19). Following subtotal nephrectomy (25) or renal transplant rejection (20) as well as left ventricular remodeling (38, 41), VEGF-C produced by inflammatory macrophages induces massive lymphangiogenesis, and angiotensin II promotes monocyte and macrophage recruitment (28). Taken together, a vicious circle of fibrosis-induced lymphangiogenesis and inflammation promoted by lymphatic capillaries propagates fibrosis.

Glomerular podoplanin loss was related to inflammatory infiltration in the surrounding tubulointerstitium or was related to sclerosis of the glomeruli. Glomerular podoplanin loss may be an early marker of glomerular damage, even before the appearance of fibrotic matrix deposition in glomeruli. Loss of podoplanin from podocytes in glomerular disease has been described previously (4). Loss of podoplanin could be associated with proteinuria, similarly to the effect of anti-podoplanin IgG injection reported earlier (24). Our study underlines the important role of podocytes in the hyperfiltration-induced glomerular sclerosis.

Conclusions. The known beneficial effects of ACEi therapy in reducing allograft fibrosis may be explained in part by reducing glomerular capillary pressure and consequent podocyte damage. Podoplanin loss in glomeruli is a marker of podocyte damage, which ultimately causes proteinuria. Proteinuria is thought to initiate and sustain tubulointerstitial fibrosis accompanied with blood capillary rarefaction. Rarefaction correlated with fibrosis. The amelioration of rarefaction by ACEi therapy suggests an etiological role of rarefaction dependent on hypoxia in the progression of fibrosis (Fig. 8). On the other hand, proteinuria and edema of the fibrotic tissue

stimulate lymphangiogenesis. The observation of lymphatic capillaries with T and B lymphocytes at sites of fibrosis and the fact that the extent of lymphangiogenesis correlated with proteinuria and fibrosis suggest an etiological role of lymphatic capillary neoangiogenesis in inflammation and fibrosis. Neither focal infiltration nor lymphatic capillary numbers progressed significantly during the observation period, suggesting a self-limiting process in this inflammation. We hypothesize that lymphatic capillaries may have a regulatory role contributing to the self-limiting nature of the inflammation.

ACKNOWLEDGMENTS

We are grateful for the technical assistance of Katalin Nagy-Bojarszky (AKH, Vienna) and Mária Godó and statistical analysis and proofreading of Gábor Szénási (Semmelweis, Budapest).

GRANTS

Support was provided to P. Hamar from the Hungarian Research Fund: OTKA ANN-110810, SNN-114619, the Austrian-Hungarian Foundation for researcher exchange (OMAA-AÖU: 90öu15), and Bolyai Scholarship of the Hungarian Academy of Sciences and Merit Award of Semmelweis University.

DISCLOSURES

No conflicts of interest, financial or otherwise, are declared by the authors.

AUTHOR CONTRIBUTIONS

P.H. and D.K. conception and design of research; P.H. and D.K. performed experiments; P.H. and D.K. analyzed data; P.H. and D.K. interpreted results of experiments; P.H. prepared figures; P.H. drafted manuscript; P.H. and D.K. edited and revised manuscript; P.H. and D.K. approved final version of manuscript.

REFERENCES

- Amann K, Haas CS. What you should know about the work-up of a renal biopsy. *Nephrol Dial Transplant* 21: 1157–1161, 2006.
- Ameer OZ, Salman IM, Avolio AP, Phillips JK, Butlin M. Opposing changes in thoracic and abdominal aortic biomechanical properties in rodent models of vascular calcification and hypertension. *Am J Physiol Heart Circ Physiol* 307: H143–H151, 2014.
- Ashpole NM, Warrington JP, Mitschelen MC, Yan H, Sosnowska D, Gautam T, Farley JA, Csiszar A, Ungvari Z, Sonntag WE. Systemic influences contribute to prolonged microvascular rarefaction after brain irradiation: A role for endothelial progenitor cells. *Am J Physiol Heart Circ Physiol* 307: H858–H868, 2014.
- Breiteneder-Geleff S, Matsui K, Soleiman A, Meraner P, Poczewski H, Kalt R, Schaffner G, Kerjaschki D. Podoplanin, novel 43-kd membrane protein of glomerular epithelial cells, is down-regulated in puromycin nephrosis. *Am J Pathol* 151: 1141–1152, 1997.
- Brown NJ, Vaughan DE. Angiotensin-converting enzyme inhibitors. *Circulation* 97: 1411–1420, 1998.
- Chakraborty S, Zawieja SD, Wang W, Lee Y, Wang YJ, von der Weid PY, Zawieja DC, Muthuchamy M. Lipopolysaccharide modulates neutrophil recruitment and macrophage polarization on lymphatic vessels and impairs lymphatic function in rat mesentery. *Am J Physiol Heart Circ Physiol* 309: H2042–H2057, 2015.
- Chappell MC. Biochemical evaluation of the renin-angiotensin system: The good, bad, and absolute? *Am J Physiol Heart Circ Physiol* 310: H137–H152, 2016.
- Clements ME, Chaber CJ, Ledbetter SR, Zuk A. Increased cellular senescence and vascular rarefaction exacerbate the progression of kidney fibrosis in aged mice following transient ischemic injury. *PLoS One* 8: e70464, 2013.
- D'Souza KM, Biwer LA, Madhavpeddi L, Ramaiah P, Shahid W, Hale TM. Persistent change in cardiac fibroblast physiology after transient ACE inhibition. *Am J Physiol Heart Circ Physiol* 309: H1346–H1353, 2015.
- Datar SA, Gong W, He Y, Johengen M, Kameny RJ, Raff GW, Maltepe E, Oishi PE, Fineman JR. Disrupted NOS signaling in lym-

- phatic endothelial cells exposed to chronically increased pulmonary lymph flow. *Am J Physiol Heart Circ Physiol* 311: H137–H145, 2016.
11. Edwards KD, Curtis EA, Stoker LM. One-day renal function testing in normal rats and in cases of experimentally-induced analgesic nephropathy, nephrocalcinosis and nephrotic syndrome. *Nephron* 8: 235–245, 1971.
 12. Fligny C, Duffield JS. Activation of pericytes: Recent insights into kidney fibrosis and microvascular rarefaction. *Curr Opin Rheumatol* 25: 78–86, 2013.
 13. Ghanta S, Cuzzone DA, Torrisi JS, Albano NJ, Joseph WJ, Savetsky IL, Gardener JC, Chang D, Zampell JC, Mehrara BJ. Regulation of inflammation and fibrosis by macrophages in lymphedema. *Am J Physiol Heart Circ Physiol* 308: H1065–H1077, 2015.
 14. Hamar P, Liptak P, Heemann U, Ivanyi B. Ultrastructural analysis of the Fisher to Lewis rat model of chronic allograft nephropathy. *Transpl Int* 18: 863–870, 2005.
 15. Hamar P, Liu S, Viklicky O, Szabo A, Muller V, Heemann U. Cyclosporine A and azathioprine are equipotent in chronic kidney allograft rejection. *Transplantation* 69: 1290–1295, 2000.
 16. Hamar P, Peti-Peterdi J, Razga Z, Kovacs G, Heemann U, Rosivall L. Coinhibition of immune and renin-angiotensin systems reduces the pace of glomerulosclerosis in the rat remnant kidney. *J Am Soc Nephrol* 10, Suppl 11: S234–S238, 1999.
 17. Hamar P, Szabo A, Muller V, Heemann U. The involvement of activated T cells and growth-factor production in the early and late phase of chronic kidney allograft nephropathy in rats. *Transpl Int* 15: 446–454, 2002.
 18. Jubair S, Li J, Dehlin HM, Manteufel EJ, Goldspink PH, Levick SP, Janicki JS. Substance P induces cardioprotection in ischemia-reperfusion via activation of AKT. *Am J Physiol Heart Circ Physiol* 309: H676–H684, 2015.
 19. Jung YJ, Lee AS, Nguyen-Thanh T, Kang KP, Lee S, Jang KY, Kim MK, Kim SH, Park SK, Kim W. Hyaluronan-induced VEGF-C promotes fibrosis-induced lymphangiogenesis via Toll-like receptor 4-dependent signal pathway. *Biochem Biophys Res Commun* 466: 339–345, 2015.
 20. Kerjaschki D, Huttary N, Raab I, Regele H, Bojarski-Nagy K, Bartel G, Krober SM, Greinix H, Rosenmaier A, Karhofer A, Wick N, Mazal PR. Lymphatic endothelial progenitor cells contribute to de novo lymphangiogenesis in human renal transplants. *Nat Med* 12: 230–234, 2006.
 21. Lammoglia GM, Van Zandt CE, Galvan DX, Orozco JL, Dellinger MT, Rutkowski JM. Hyperplasia, de novo lymphangiogenesis, and lymphatic regression in mice with tissue-specific, inducible overexpression of murine VEGF-D. *Am J Physiol Heart Circ Physiol* 311: H384–H394, 2016.
 22. Li Y, Kinzenbaw DA, Modrick ML, Pewe LL, Faraci FM. Context-dependent effects of SOCS3 in angiotensin II-induced vascular dysfunction and hypertension in mice: Mechanisms and role of bone marrow-derived cells. *Am J Physiol Heart Circ Physiol* 311: H146–H156, 2016.
 23. Lynch LL, Mendez U, Waller AB, Gillette AA, Guillory RJ, 2nd, Goldman J. Fibrosis worsens chronic lymphedema in rodent tissues. *Am J Physiol Heart Circ Physiol* 308: H1229–H1236, 2015.
 24. Matsui K, Breiteneder-Geleff S, Kerjaschki D. Epitope-specific antibodies to the 43-kD glomerular membrane protein podoplanin cause proteinuria and rapid flattening of podocytes. *J Am Soc Nephrol* 9: 2013–2026, 1998.
 25. Matsui K, Nagy-Bojarsky K, Laakkonen P, Krieger S, Mechtler K, Uchida S, Geleff S, Kang DH, Johnson RJ, Kerjaschki D. Lymphatic microvessels in the rat remnant kidney model of renal fibrosis: Aminopeptidase p and podoplanin are discriminatory markers for endothelial cells of blood and lymphatic vessels. *J Am Soc Nephrol* 14: 1981–1989, 2003.
 26. Mayer G. Capillary rarefaction, hypoxia, VEGF and angiogenesis in chronic renal disease. *Nephrol Dial Transplant* 26: 1132–1137, 2011.
 27. Mezzano SA, Ruiz-Ortega M, Egido J. Angiotensin II and renal fibrosis. *Hypertension* 38: 635–638, 2001.
 28. Moore JP, Vinh A, Tuck KL, Sakkal S, Krishnan SM, Chan CT, Lieu M, Samuel CS, Diep H, Kemp-Harper BK, Tare M, Ricardo SD, Guzik TJ, Sobey CG, Drummond GR. M2 macrophage accumulation in the aortic wall during angiotensin II infusion in mice is associated with fibrosis, elastin loss, and elevated blood pressure. *Am J Physiol Heart Circ Physiol* 309: H906–H917, 2015.
 29. Muller V, Hamar P, Szabo A, Vogelsang M, Philipp T, Heemann U. In vivo migration of lymphocytes in chronically rejecting rat kidney allografts. *Transpl Int* 12: 145–151, 1999.
 30. Pachon RE, Scharf BA, Vatner DE, Vatner SF. Best anesthetics for assessing left ventricular systolic function by echocardiography in mice. *Am J Physiol Heart Circ Physiol* 308: H1525–H1529, 2015.
 31. Remuzzi A, Sangalli F, Macconi D, Tomasoni S, Cattaneo I, Rizzo P, Bonandrini B, Bresciani E, Longaretti L, Gagliardini E, Conti S, Benigni A, Remuzzi G. Regression of renal disease by angiotensin II antagonism is caused by regeneration of kidney vasculature. *J Am Soc Nephrol* 27: 699–705, 2016.
 32. Schmid C, Heemann U, Tilney NL. Retransplantation reverses mononuclear infiltration but not myointimal proliferation in a rat model of chronic cardiac allograft rejection. *Transplantation* 61: 1695–1699, 1996.
 33. Shi Y, Tu Z, Bao J, Sun H, Wang W, Luo G, Li S, Li Y, Bu H. Urinary connective tissue growth factor increases far earlier than histopathological damage and functional deterioration in early chronic renal allograft injury. *Scand J Urol Nephrol* 43: 390–399, 2009.
 34. Solez K, Colvin RB, Racusen LC, Haas M, Sis B, Mengel M, Halloran PF, Baldwin W, Banfi G, Collins AB, Cosio F, David DS, Drachenberg C, Einecke G, Fogo AB, Gibson IW, Glotz D, Iskandar SS, Kraus E, Lerut E, Mannon RB, Mihatsch M, Nankivell BJ, Nickleleit V, Papadimitriou JC, Randhawa P, Regele H, Renaudin K, Roberts I, Seron D, Smith RN, Valente M. Banff 07 classification of renal allograft pathology: Updates and future directions. *Am J Transplant* 8: 753–760, 2008.
 35. Szabo A, Lutz J, Schleimer K, Antus B, Hamar P, Philipp T, Heemann U. Effect of angiotensin-converting enzyme inhibition on growth factor mRNA in chronic renal allograft rejection in the rat. *Kidney Int* 57: 982–991, 2000.
 36. Thomas CM, Yong QC, Rosa RM, Seqqat R, Gopal S, Casarini DE, Jones WK, Gupta S, Baker KM, Kumar R. Cardiac-specific suppression of NF- κ B signaling prevents diabetic cardiomyopathy via inhibition of the renin-angiotensin system. *Am J Physiol Heart Circ Physiol* 307: H1036–H1045, 2014.
 37. Toldo S, Mezzaroma E, O'Brien L, Marchetti C, Seropian IM, Voelkel NF, Van Tassel BW, Dinarello CA, Abbate A. Interleukin-18 mediates interleukin-1-induced cardiac dysfunction. *Am J Physiol Heart Circ Physiol* 306: H1025–H1031, 2014.
 38. Yang GH, Zhou X, Ji WJ, Zeng S, Dong Y, Tian L, Bi Y, Guo ZZ, Gao F, Chen H, Jiang TM, Li YM. Overexpression of VEGF-C attenuates chronic high salt intake-induced left ventricular maladaptive remodeling in spontaneously hypertensive rats. *Am J Physiol Heart Circ Physiol* 306: H598–H609, 2014.
 39. Yazdani S, Hijmans RS, Poosti F, Dam W, Navis G, van Goor H, van den Born J. Targeting tubulointerstitial remodeling in proteinuric nephropathy in rats. *Dis Model Mech* 8: 919–930, 2015.
 40. Yazdani S, Poosti F, Kramer AB, Mirkovic K, Kwakernaak AJ, Hovingh M, Slagman MC, Sjollem KA, de Borst MH, Navis G, van Goor H, van den Born J. Proteinuria triggers renal lymphangiogenesis prior to the development of interstitial fibrosis. *PLoS One* 7: e50209, 2012.
 41. Zhao T, Zhao W, Meng W, Liu C, Chen Y, Sun Y. Vascular endothelial growth factor-C: Its unrevealed role in fibrogenesis. *Am J Physiol Heart Circ Physiol* 306: H789–H796, 2014.
 42. Zuurbier CJ, Koeman A, Janssen BJ. Letter to the editor: Ketamine-only versus isoflurane effects on murine cardiac function: Comparison at similar depths of anesthesia? *Am J Physiol Heart Circ Physiol* 309: H2160, 2015.